# 2

# Digital Backward Propagation: A Technique to Compensate Fiber Dispersion and Non-Linear Impairments

Rameez Asif, Chien-Yu Lin and Bernhard Schmauss
*Chair of Microwave Engineering and High Frequency Technology (LHFT),*
*Erlangen Graduate School in Advanced Optical Technologies (SAOT),*
*Friedrich-Alexander University of Erlangen-Nuremberg (FAU),*
*Cauerstr. 9, (91058) Erlangen*
*Germany*

## 1. Introduction

Recent numerical and experimental studies have shown that coherent optical QPSK (CO-QPSK) is the promising candidate for next-generation 100Gbit/s Ethernet (100 GbE) (Fludger et al., 2008). Coherent detection is considered efficient along with digital signal processing (DSP) to compensate many linear effects in fiber propagation i.e. chromatic dispersion (CD) and polarization-mode dispersion (PMD) and also offers low required optical signal-to-noise ratio (OSNR). Despite of fiber dispersion and non-linearities which are the major limiting factors, as illustrated in Fig. 1, optical transmission systems are employing higher order modulation formats in order to increase the spectral efficiency and thus fulfil the ever increasing demand of capacity requirements (Mitra et al., 2001). As a result of which compensation of dispersion and non-linearities (NL), i.e. self-phase modulation (SPM), cross-phase modulation (XPM) and four-wave mixing (FWM), is a point of high interest these days.

Various methods of compensating fiber transmission impairments have been proposed in recent era by implementing all-optical signal processing. It is demonstrated that the fiber dispersion can be compensated by using the mid-link spectral inversion method (MLSI) (Feiste et al., 1998; Jansen et al., 2005). MLSI method is based on the principle of optical phase conjugation (OPC). In a system based on MLSI, no in-line dispersion compensation is needed. Instead in the middle of the link, an optical phase conjugator inverts the frequency spectrum and phase of the distorted signals caused by chromatic dispersion. As the signals propagate to the end of the link, the accumulated spectral phase distortions are reverted back to the value at the beginning of the link if perfect symmetry of the link is assured. In (Marazzi et al., 2009), this technique is demonstrated for real-time implementation in 100Gbit/s POLMUX-DQPSK transmission.

Another all-optical method to compensate fiber transmission impairments is proposed in (Cvecek et al., 2008; Sponsel et al., 2008) by using the non-linear amplifying loop mirror (NALM). In this technique the incoming signal is split asymmetrically at the fiber coupler

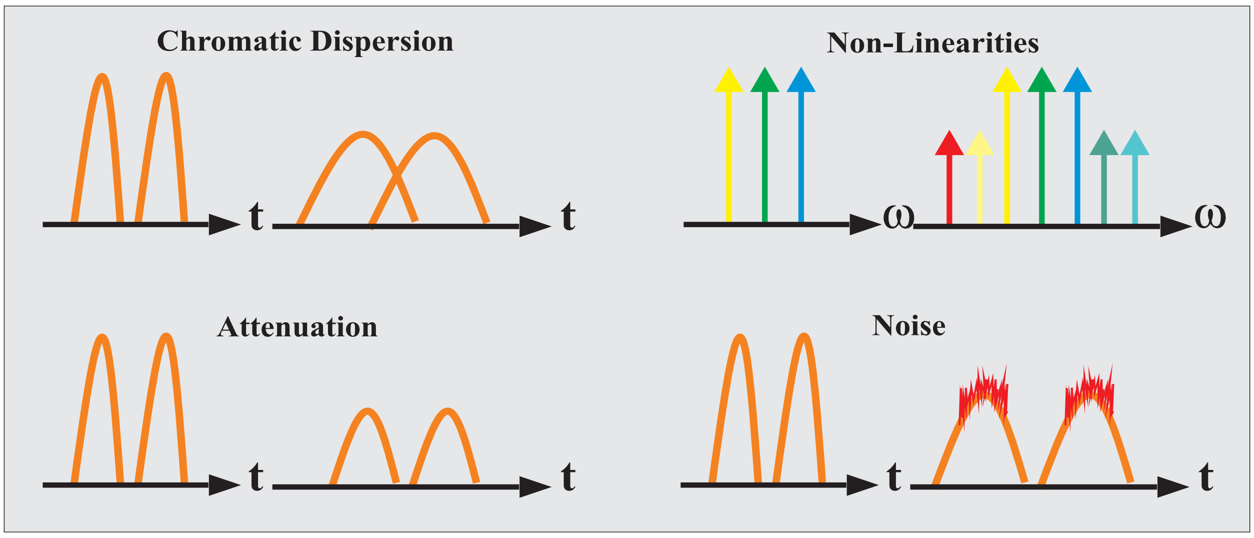


Fig. 1. Optical fiber transmission impairments.

into two counter-propagating signals. The weaker partial pulse passes first through the EDFA where it is amplified by about 20dB. It gains a significant phase shift due to self-phase modulation (Stephan et al., 2009) in the highly non-linear fiber (HNLF). The initially stronger pulse propagates through the fiber before it is amplified, so that the phase shift in the HNLF is marginal. At the output coupler the strong partial pulse with almost unchanged phase and the weak partial pulse with input-power-dependent phase shift interfere. The first, being much stronger, determines the phase of the output signal and therefore ensures negligible phase distortions.

Various investigations have been also been reported to examine the effect of optical link design (Lin et al., 2010a; Randhawa et al., 2010; Tonello et al., 2006) on the compensation of fiber impairments. However, the applications of all-optical methods are expensive, less flexible and less adaptive to different configurations of transmission. On the other hand with the development of proficient real time digital signal processing (DSP) techniques and coherent receivers, finite impulse response (FIR) filters become popular and have emerged as the promising techniques for long-haul optical data transmission. After coherent detection the signals, known in amplitude and phase, can be sampled and processed by DSP to compensate fiber transmission impairments.

DSP techniques are gaining increasing importance as they allow for robust long-haul transmission with compensation of fiber impairments at the receiver (Li, 2009; Savory et al., 2007). One major advantage of using DSP after sampling of the outputs from a phase-diversity receiver is that hardware optical phase locking can be avoided and only digital phase-tracking is needed (Noe, 2005; Taylor, 2004). DSP algorithms can also be used to compensate chromatic dispersion (CD) and polarization-mode dispersion (PMD) (Winters, 1990). It is depicted that for a symbol rate of $\tau$, a $\frac{\tau}{2}$ tap delay finite impulse response (FIR) filter may be used to reverse the effect of fiber chromatic dispersion (Savory et al., 2006). The number of FIR taps increases linearly with increasing accumulated dispersion i.e the number of taps required to compensate 1280 ps/nm of dispersion is approximately 5.8 (Goldfarb et al., 2007). At long propagation distances, the extra power consumption required for this task becomes significant. Moreover, a longer FIR filter introduces a longer delay and requires more area on a DSP circuitry.

Alternatively, infinite impulse response (IIR) filters can used (Goldfarb et al., 2007) to reduce the complexity of the DSP circuit.
However, with the use of higher order modulation formats, i.e QPSK and QAM, to meet the capacity requirements, it becomes vital to compensate non-linearities along with the fiber dispersion. Due to this non-linear threshold point (NLT) of the transmission system can be improved and more signal power can be injected in the system to have longer transmission distances. In (Geyer et al., 2010) a low complexity non-linear compensator scheme with automatic control loop is introduced. The proposed simple non-linear compensator requires considerably lower implementation complexity and can blindly adapt the required coefficients. In uncompensated links, the simple scheme is not able to improve performance, as the non-linear distortions are distributed over different amounts of CD-impairment. Nevertheless the scheme might still be useful to compensate possible non-linear distortions of the transmitter. In transmission links with full in-line compensation the compensator provides 1dB additional noise tolerance. This makes it useful in 10Gbit/s upgrade scenarios where optical CD compensation is still present. Another promising electronic method, investigated in higher bit-rate transmissions and for diverse dispersion mapping, is the digital backward propagation (DBP), which can jointly mitigate dispersion and non-linearities. The DBP algorithm can be implemented numerically by solving the inverse non-linear Schrödinger equation (NLSE) using split-step Fourier method (SSFM) (Ip et al., 2008). This technique is an off-line signal processing method. The limitation so far for its real-time implementation is the complexity of the algorithm (Yamazaki et al., 2011). The performance of the algorithm is dependent on the calculation steps ($h$), to estimate the transmission link parameters with accuracy, and on the knowledge of transmission link design.
In this chapter we give a detailed overview on the advancements in DBP algorithm based on different types of mathematical models. We discuss the importance of optimized step-size selection for simplified and computationally efficient algorithm of DBP.

## 2. State of the art

Pioneering concepts on backward propagation have been reported in articles of (Pare et al., 1996; Tsang et al., 2003). In (Tsang et al., 2003) backward propagation is demonstrated as a numerical technique for reversing femtosecond pulse propagation in an optical fiber, such that given any output pulse it is possible to obtain the input pulse shape by numerically undoing all dispersion and non-linear effects. Whereas, in (Pare et al., 1996) a dispersive medium with a negative non-linear refractive-index coefficient is demonstrated to compensate the dispersion and the non-linearities. Based on the fact that signal propagation can be interpreted by the non-linear Schrödinger equation (NLSE) (Agrawal, 2001). The inverse solution i.e. backward propagation, of this equation can numerically be solved by using split-step Fourier method (SSFM). So backward propagation can be implemented digitally at the receiver (see section 3.2 of this chapter). In digital domain, first important investigations (Ip et al., 2008; Li et al., 2008) are reported on compensation of transmission impairments by DBP with modern-age optical communication systems and coherent receivers. Coherent detection plays a vital role for DBP algorithm as it provides necessary information about the signal phase. In (Ip et al., 2008) 21.4Gbit/s RZ-QPSK transmission model over 2000km single mode fiber (SMF) is used to investigate the role of dispersion mapping, sampling ratio and multi-channel transmission. DBP is implemented by using a asymmetric split-step Fourier method (A-SSFM). In A-SSFM method each calculation step is solved by linear operator ($\hat{D}$)

followed by a non-linear operator ($\hat{N}$) (see section 3.2.1 of this chapter). In this investigation the results depict that the efficient performance of DBP algorithm can be obtained if there is no dispersion compensating fiber (DCF) in the transmission link. This is due to the fact that in the fully compensated post-compensation link the pulse shape is restored completely at the input of the transmission fiber in each span. This reduces the system efficiency due to the maximized accumulation of non-linearities and the high signal-ASE (amplified spontaneous emission) interaction leading to non-linear phase noise (NLPN). So it is beneficial to fully compensate dispersion digitally at the receiver by DBP. The second observation in this article is about the oversampling rate which improves system performance by DBP.

A number of investigations with diverse transmission configurations have been done with coherent detection and split-step Fourier method (SSFM) (Asif et al., 2010; Mateo et al., 2011; Millar et al., 2010; Mussolin et al., 2010; Rafique et al., 2011a; Yaman et al., 2009). The results in these articles shows efficient mitigation of CD and NL. In (Asif et al., 2010) the performance of DBP is investigated for heterogeneous type transmission links which contain mixed spans of single mode fiber (SMF) and non-zero dispersion shifted fiber (NZDSF). The continuous growth of the next generation optical networks are expected to render telecommunication networks particularly heterogeneous in terms of fiber types. Efficient compensation of fiber transmission impairments is shown with different span configurations as well as with diverse dispersion mapping.

All the high capacity systems are realized with wavelength-division-multiplexed (WDM) to transmit multiple-channels on a single fiber with high spectral efficiency. The performance in these systems are limited by the inter-channel non-linearities (XPM,FWM) due to the interaction of neighbouring channels. The performance of DBP is evaluated for WDM systems in several articles (Gavioli et al., 2010; Li et al., 2008; Poggiolini et al., 2011; Savory et al., 2010). In (Savory et al., 2010) 112Gbit/s DP-QPSK transmission system is examined and investigations demonstrate that the non-linear compensation algorithm can increase the reach by 23% in a 100GHz spacing WDM link compared to 46% for the single-channel case. When the channel spacing is reduced to 50GHz, the reach improvement is minimal due to the uncompensated inter-channel non-linearities. Whereas, in (Gavioli et al., 2010; Poggiolini et al., 2011) the same-capacity and bandwidth-efficiency performance of DBP is demonstrated in a ultra-narrow-spaced 10 channel 1.12Tbit/s D-WDM long haul transmission. Investigations show that optimum system performance using DBP is obtained by using 2, 4 and 8 steps per fiber span for 14GBaud, 28GBuad and 56GBaud respectively. To overcome the limitations by inter-channel non-linearities on the performance of DBP (Mateo et al., 2010; 2011) proposed improved DBP method for WDM systems. This modification is based on including the effect of inter-channel walk-off in the non-linear step of SSFM. The algorithm is investigated in a 100Gbit/s per channel 16QAM transmission over 1000km of NZDSF type fiber. The results are compared for 12, 24 and 36 channels spaced at 50GHz to evaluate the impact of channel count on the DBP algorithm. While self-phase modulation (SPM) compensation is not sufficient in DWDM systems, XPM compensation is able to increase the transmission reach by a factor of 2.5 by using this DBP method. The results depicts efficient compensation of cross-phase modulation (XPM) and the performance of DBP is improved for WDM systems.

Polarization multiplexing (POLMUX) (Evangelides et al., 1992; Iwatsuki et al., 1993) opens a total new era in optical communication systems (Fludger et al., 2008) which doubles the capacity of a wavelength channel and the spectral efficiency by transmitting two signals via orthogonal states of polarization (SOPs). Although POLMUX is considered interesting for increasing the transmitted capacity, it suffers from decreased PMD tolerance (Nelson et al., 2000; 2001) and increased polarization induced cross-talk (X-Pol), due to the polarization-sensitive detection (Noe et al., 2001) used to separate the POLMUX channels. Previous investigations on DBP demonstrate the results for the WDM channels having the same polarization and solving the scaler NLSE equation is adequate. In (Yaman et al., 2009) it is depicted that the same principles can be applied to compensate fiber transmission impairments by using DBP but a much more advanced form of NLSE should be used which includes two orthogonal polarization states ($E_x$ and $E_y$), i.e. Manakov equation. Polarization mode dispersion (PMD) is considered negligible during investigation. In this article the results depict that back-to-back performance for the central channel corresponds to a Q value of 20.6 dB. When only dispersion compensation is applied it results in a Q value of 3.9 dB. The eye-diagram is severely degraded and clearly dispersion is not the only source of impairment. Whereas, when DBP algorithm is applied the system observed a Q value of 12.6 dB. The results clearly shows efficient compensation of CD and NL by using the DBP algorithm. In (Mussolin et al., 2010; Rafique et al., 2011b) 100Gbit/s dual-polarization (DP) transmission systems are investigated with advanced modulation formats i.e. QPSK and QAM.

Another modification in recent times in conventional DBP algorithm is the optimization of non-linear operator calculation point ($r$). It is demonstrated that DBP in a single-channel transmission (Du et al., 2010; Lin et al., 2010b) can be improved by using modified split-step Fourier method (M-SSFM). Modification is done by shifting the non-linear operator calculation point $Nlpt$ ($r$) along with the optimization of dispersion $D$ and non-linear coefficient $\gamma$ to get the optimized system performance (see section 3.2.2 of this chapter). The modification in this non-linear operator calculation point is necessary due to the fact that non-linearities behave differently for diverse parameters of transmission, i.e. signal input launch power and modulation formats, and hence also due to precise estimation of non-linear phase shift $\phi_{NL}$ from span to span. The concept of filtered DBP (F-DBP) (Du et al., 2010) is also presented along with the optimization of non-linear point (see section 3.2.3 of this chapter). The system performance is improved through F-DBP by using a digital low-pass-filter (LPF) in each DBP step to limit the bandwidth of the compensating waveform. In this way we can optimize the compensation of low frequency intensity fluctuations without overcompensating for the high frequency intensity fluctuations. In (Du et al., 2010) the results depict that with four backward propagation steps operating at the same sampling rate as that required for linear equalizers, the Q at the optimal launch power was improved by 2 dB and 1.6 dB for single wavelength CO-OFDM and CO-QPSK systems, respectively, in a 3200 km (40x80km) single-mode fiber link, with no optical dispersion compensation.

Recent investigations (Ip et al., 2010; Rafique et al., 2011b) show the promising impact of DBP on OFDM transmission and higher order modulation formats, up to 256-QAM. However actual implementation of the DBP algorithm is now-a-days extremely challenging due to its complexity. The performance is mainly dependent on the computational step-size ($h$) (Poggiolini et al., 2011; Yamazaki et al., 2011) for WDM and higher baud-rate transmissions. In order to reduce the computational efforts of the algorithm by increasing the step-size (i.e. reducing the number of DBP calculation steps per fiber span), ultra-low-loss-fiber (ULF) is used (Pardo et al., 2011) and a promising method called correlated DBP (CBP) (Li et al., 2011; Rafique et al., 2011c) has been introduced (see section 4.1 of this chapter). This method takes into account the correlation between adjacent symbols at a given instant using a weighted-average approach, and an optimization of the position of non-linear compensator

stage. In (Li et al., 2011) the investigations depict the results in 100GHz channel spaced DP-QPSK transmission and multi-span DBP shows a reduction of DBP stages upto 75%. While in (Rafique et al., 2011c) the algorithm is investigated for single channel DP-QPSK transmission. In this article upto 80% reduction in required back-propagation stages is shown to perform non-linear compensation in comparison to the standard back-propagation algorithm.
In the aforementioned investigations there is a trade-off relationship between achievable improvement and algorithm complexity in the DBP. Therefore DBP algorithms with higher improvement in system performance as compared to conventional methods are very attractive. Due to this fact simplification of the DBP model to efficiently describe fiber transmission especially for POLMUX signals and an estimation method to precisely optimize parameters are the keys for its future cost-effective implementation. By keeping in mind that existing DBP techniques are implemented with constant step-size SSFM methods. The use of these methods, however, need the optimization of $D$ , $\gamma$ and $r$ for efficient mitigation of CD and NL. In (Asif et al., 2011) numerical investigation for the first time on logarithmic step-size distribution to explore the simplified and efficient implementation of DBP using SSFM is done (see section 3.2.4 of this chapter). The basic motivation of implementing logarithmic step-size relates to the fact of exponential decay of signal power and thus NL phase shift in the beginning sections of each fiber span. The algorithm is investigated in N-channel 112Gbit/s/ch DP-QPSK transmission (a total transmission capacity of 1.12Tbit/s) over 2000km SMF with no in-line optical dispersion compensation. The results depict enhanced system performance of DP-QPSK transmission, i.e. efficient mitigation of fiber transmission impairments, especially at higher baud rates. The benefit of the logarithmic step-size is the reduced complexity as the same forward propagation parameters can be used in DBP without optimization and computational time which is less than conventional M-SSFM based DBP.
The advancements in DBP algorithm till date are summarized in Appendix A. The detailed theory of split-step methods and the effect of step-size selection is explained in the following sections.

## 3. Non-linear Schrödinger equation (NLSE)

The propagation of optical signals in the single mode fiber (SMF) can be interpreted by the Maxwell's equations. It can mathematically be given as in the form of a wave equation as in Eq. 1 (Agrawal, 2001).

$$\bigtriangledown^2 E = \frac{1}{c^2}\frac{\partial^2 E}{\partial^2 t} - \mu_0 \frac{\partial^2 P(E)}{\partial^2 t} \tag{1}$$

Whereas, $E$ is the electric field, $\mu_0$ is the vacuum permeability, $c$ is the speed of light and $P$ is the polarization field. At very weak optical powers, the induced polarization has a linear relationship with $E$ such that;

$$P_L(r,t) = \varepsilon_0 \int_{-\propto}^{\propto} x^{(1)}(t-\grave{t}) \cdot E(r,\grave{t})d\grave{t} \tag{2}$$

Where $\varepsilon_0$ is the vacuum permittivity and $x^{(1)}$ is the first order susceptibility. To consider non-linearities in the system, the Eq. 2 can be re-written as illustrated in Eq. 3 (Agrawal, 2001).

$$P(r,t) = P_L(r,t) + P_{NL}(r,t) \tag{3}$$

Whereas, $P_{NL}(r,t)$ is the non-linear part of polarization. Eq. 3 can be used to solve Eq. 1 to derive the propagation equation in non-linear dispersive fibers with few simplifying assumptions. First, $P_{NL}$ is treated as a small perturbation of $P_L$ and the polarization field is maintained throughout the whole propagation path. Another assumption is that the index difference between the core and cladding is very small and the center frequency of the wave is assumed to be much greater than the spectral width of the wave which is also called as quasi-monochromatic assumption. The quasi-monochromatic assumption is the analogous to low-pass equivalent modelling of bandpass electrical systems and is equivalent to the slowly varying envelope approximation in the time domain. Finally, the propagation constant, $\beta(\omega)$, is approximated by a few first terms of Taylor series expansion about the carrier frequency, $\omega_0$, that can be given as;

$$\beta(\omega) = \beta_0 + (\omega - \omega_0)\beta_1 + \frac{1}{2}(\omega - \omega_0)^2\beta_2 + \frac{1}{6}(\omega - \omega_0)^3\beta_3 + ....... \tag{4}$$

Whereas;

$$\beta_n = \left[\frac{d^n\beta}{d\omega^n}\right]_{\omega=\omega_0} \tag{5}$$

The second order propagation constant $\beta_2[ps^2/km]$, accounts for the dispersion effects in the optical fibers communication systems. Depending on the sign of the $\beta_2$, the dispersion region can be classified into two parts as, normal($\beta_2 > 0$) and anomalous ($\beta_2 < 0$). Qualitatively, in the normal-dispersion region, the higher frequency components of an optical signal travel slower than the lower frequency components. In the anomalous dispersion region it occurs vice-versa. Fiber dispersion is often expressed by another parameter, $D[ps/(nm.km)]$, which is called as dispersion parameter. $D$ is defined as $D = \frac{d}{d\lambda}\left[\frac{1}{v_g}\right]$ and the mathematical relationship between $\beta_2$ and $D$ is given in (Agrawal, 2001), as;

$$\beta_2 = -\frac{\lambda^2}{2\pi c}D \tag{6}$$

Where $\lambda$ is the wavelength of the propagating wave and $v_g$ is the group velocity. The cubic and the higher order terms in Eq. 4 are generally negligible as long as the quasi-monochromatic assumption remains valid. However, when the center wavelength of an optical signal is near the zero-dispersion wavelength, as for broad spectrum of the signals, (that is $\beta \approx 0$) then the $\beta_3$ terms should be included.

If the input electric field is assumed to propagate in the $+z$ direction and is polarized in the $x$ direction Eq. 1 can be re-written as;

$$\begin{aligned} \frac{\partial}{\partial z}E(z,t) = -\frac{\alpha}{2}E(z,t) & \qquad \text{(linear attenuation)} \\ +j\frac{\beta_2}{2}\frac{\partial^2}{\partial^2 t}E(z,t) & \qquad \text{(second order dispersion)} \end{aligned}$$

$$
\begin{aligned}
&+\frac{\beta_3}{6}\frac{\partial^3}{\partial^3 t}E(z,t) && \text{(third order dispersion)}\\
&-j\gamma|E(z,t)|^2E(z,t) && \text{(Kerr effect)}\\
&+j\gamma T_R\frac{\partial}{\partial_t}|E(z,t)|^2E(z,t) && \text{(SRS)}\\
&-\frac{\partial}{\omega_0}\frac{\partial}{\partial_t}|E(z,t)|^2E(z,t) && \text{(self-steeping effect)}
\end{aligned} \tag{7}
$$

Where $E(z,t)$ is the varying slowly envelope of the electric field, $z$ is the propagation distance, $t$=$t'$-$\frac{z}{v_g}$ ($t'$= physical time, $v_g$=the group velocity at the center wavelength), $\alpha$ is the fiber loss coefficient $[1/km]$, $\beta_2$ is the second order propagation constant $[ps^2/km]$, $\beta_3$ is the third order propagation constant $[ps^3/km]$, $\gamma$=$\frac{2\pi n_2}{\lambda_0 A_{eff}}$ is the non-linear coefficient $[km^{-1}\cdot W^{-1}]$, $n_2$ is the non-linear index coefficient, $A_{eff}$ is the effective core area of the fiber, $\lambda_0$ is the center wavelength and $\omega_0$ is the central angular frequency. When the pulse width is greater than 1ps, Eq. 7 can further be simplified because the Raman effects and self-steepening effects are negligible compared to the Kerr effect (Agrawal, 2001). Mathematically the generalized form of non-linear Schrödinger equation suitable to describe the signal propagation in communication systems can be given as;

$$\frac{\partial E}{\partial z} = j\gamma|E|^2 + \left(-j\frac{\beta_2}{2}\frac{\partial^2}{\partial t^2} - \frac{\alpha}{2}\right)E = (\hat{N}+\hat{D})E \tag{8}$$

Also that $\hat{D}$ and $\hat{N}$ are termed as linear and non-linear operators as in Eq. 9.

$$\hat{N} = j\gamma|E|^2; \hat{D} = \left(-j\frac{\beta_2}{2}\frac{\partial^2}{\partial t^2} - \frac{\alpha}{2}\right) \tag{9}$$

### 3.1 Split-step Fourier method (SSFM)

As described in the previous section, it is desirable to solve the non-linear Schrödinger equation to estimate various fiber impairments occurring during signal transmission with high precision. The split-step Fourier method (SSFM) is the most popular algorithm because of its good accuracy and relatively modest computing cost.

As depicted in Eq. 8, the generalized form of NLSE contains the linear operator $\hat{D}$ and non-linear operators $\hat{N}$ and they can be expressed as in Eq. 9. When the electric field envelope, $E(z,t)$, has propagated from $z$ to $z+h$, the analytical solution of Eq. 8 can be written as;

$$E(z+h,t) = exp\big(h(\hat{N}+\hat{D})\big)\cdot E(z,t) \tag{10}$$

In the above equation $h$ is the propagation step length also called as step-size, through the fiber section. In the split-step Fourier method, it is assumed that the two operators commute with each other as in Eq. 11;

$$E(z+h,t) \approx exp\big(h(\hat{N})\big)exp\big(h(\hat{D})\big)\cdot E(z,t) \tag{11}$$

Eq.11 suggests that $E(z+h,t)$ can be estimated by applying the two operators independently. If $h$ is small, Eq.11 can give high accuracy results. The value of $h$ is usually chosen such that the maximum phase shift ($\phi_{max} = \gamma|Ep^2|h$, $Ep$=peak value of $E(z,t)$) due to the non-linear

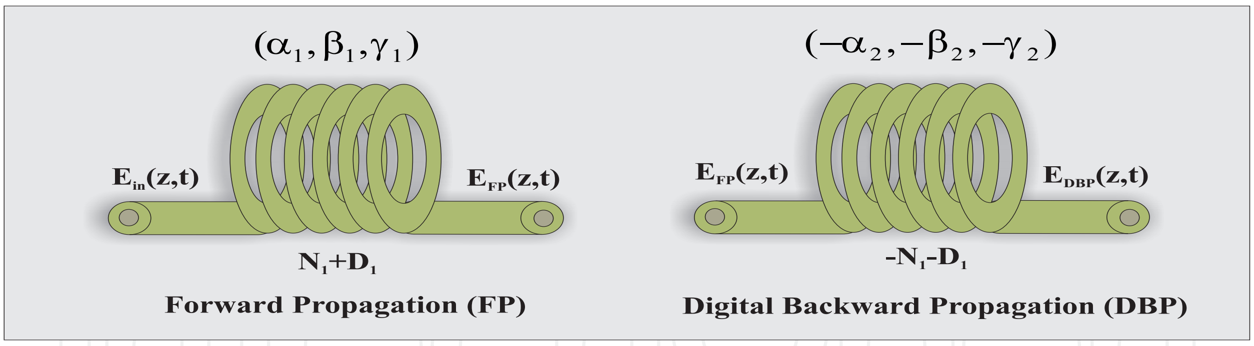


Fig. 2. Block diagram of forward propagation (FP) and digital backward propagation (DBP).

operator is below a certain value. It has been reported (Sinkin et al., 2003) that when $\phi_{max}$ is below 0.05 *rad*, the split-step Fourier method gives a good result for simulation of most optical communication systems. The simulation time of Eq.11 will greatly depend on the step-size of $h$. The block diagram of SSFM method is shown in Fig. 4.

### 3.2 Digital backward propagation (DBP)

The non-linear Schrödinger equation can be solved inversely to calculate the undistorted transmitted signal from the distorted received signal. The received signal at the receiver after transmission i.e. forward propagation (FP), is processed through a numerical model by using the negative sign with the propagation parameters i.e. dispersion $D$, non-linear coefficient $\gamma$. The method is termed as digital backward propagation (DBP) and is illustrated in Fig. 2. Mathematically inverse non-linear Schrödinger equation can be given as in Eq. 12;

$$\frac{\partial E}{\partial z} = \left(-\hat{N} - \hat{D}\right)E \tag{12}$$

Whereas; the $\hat{D}$ and $\hat{N}$ are the linear and non-linear operators respectively.

The performance of DBP algorithm mainly depends on the estimation of propagating parameters of NLSE. To numerically solve NLSE with high accuracy, split-step Fourier method (SSFM) is used as discussed in the previous section. Both the operators i.e. linear $\hat{D}$ and non-linear $\hat{N}$ are solved separately and also that linear $\hat{D}$ part is solved in frequency domain whereas non-linear $\hat{N}$ is solved in time domain. This DBP model can be implemented both on the transmitter side as well as on the receiver side. When the signal is numerically distorted at the transmitter by DBP algorithm and then this pre-distorted signal is transmitted through fiber link it is termed as transmitter side DBP (Ip et al., 2008). While in majority of the cases DBP is implemented along with the coherent receiver, it is termed as receiver side DBP (Ip et al., 2008), and as an example QPSK receiver is illustrated as in Fig. 3. In the absence of noise in the transmission link both the schemes of DBP are equivalent. As the backward propagation operates on the complex-envelope of $E(z,t)$, this algorithm in principle is applicable with any modulation format of the transmission. It should be noted that the performance of DBP is limited by the amplified spontaneous emission (ASE) noise as it is a non-deterministic noise source and cannot be back propagated (Ip et al., 2008). DBP can only take into account the deterministic impairments. In terms of step-size $h$, DBP can be categorized in 3 types: (a) sub-span step size in which multiple calculation steps are processed over a single span of fiber; (b) per-span step size which is one calculation step per fiber span and (c) multi-span step size in which one calculation step is processed over several spans of

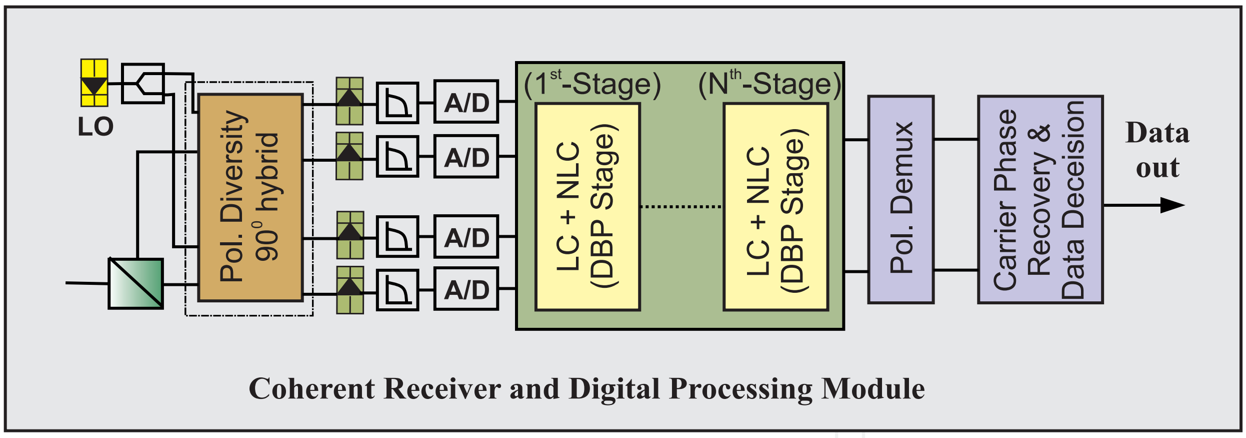


Fig. 3. Block diagram of coherent receiver with digital signal processing module of DBP (LC=linear compensation and NLC=non-linear compensation).

fiber. The SSFM methods which are used to implement the DBP algorithm are discussed in next sections.

### 3.2.1 Asymmetric and Symmetric SSFM (A-SSFM and S-SSFM)

SSFM can be implemented by using two conventional methods: asymmetric SSFM (A-SSFM) method where the linear operator ($\hat{D}$) is followed by a non-linear operator ($\hat{N}$) and symmetric SSFM (S-SSFM) method where the linear operator ($\hat{D}$) is split into two halves and is evaluated on both sides of non-linear operator ($\hat{N}$), as shown in Fig. 4. Mathematically S-SSFM can be given as in Eq. 13 and A-SSFM in Eq. 14.

$$E(z+h,t) = exp\left(\frac{h\hat{D}}{2}\right)exp\left(h\hat{N}\right)exp\left(\frac{h\hat{D}}{2}\right) \cdot E(z,t) \tag{13}$$

$$E(z+h,t) = exp\left(h\hat{D}\right)exp\left(h\hat{N}\right) \cdot E(z,t) \tag{14}$$

Two methods are adapted for computing parameters in S-SSFM (Asif et al., 2010; Ip et al., 2008). The method in which $\hat{N}(z+h)$ is calculated by initially assuming it as $\hat{N}(z)$ then estimating $E(z+h,t)$ , which enables a new value of $\hat{N}_{new}(z+h)$ and subsequently estimating $E_{new}(z+h,t)$ is termed as iterative symmetric SSFM (IS-SSFM). The other method, which is less time consuming and has fewer computations, is based on the calculation of $\hat{N}(z+h)$ at the middle of propagation $h$ is termed as non-iterative symmetric SSFM (NIS-SSFM). However computational efficiency of NIS-SSFM is better then IS-SSFM method (Asif et al., 2010).

### 3.2.2 Modified split-step Fourier method (M-SSFM)

For the modification of conventional SSFM method, (**?**) introduces a coefficient $r$ which defines the position of non-linear operator calculation point ($Nlpt$), as illustrated in Fig. 4. Typically, $r$=0 for A-SSFM and $r$=0.5 for S-SSFM. Which means that with per-span DBP compensation A-SSFM models all the fiber non-linearities as a single lumped non-linearity calculation point which is at $r$=0 (at the end of DBP fiber span) and S-SSFM models all the fiber non-linearities as a single lumped non-linearity calculation point which is at $r$=0.5. This approximation becomes less accurate particularly in case of sub-span DBP or multi-span DBP due to inter-span non-linear phase shift estimation $\phi_{NL}$, which may result in the over-compensation or under-compensation of the fiber non-linearity, reducing the mitigation of fiber impairments

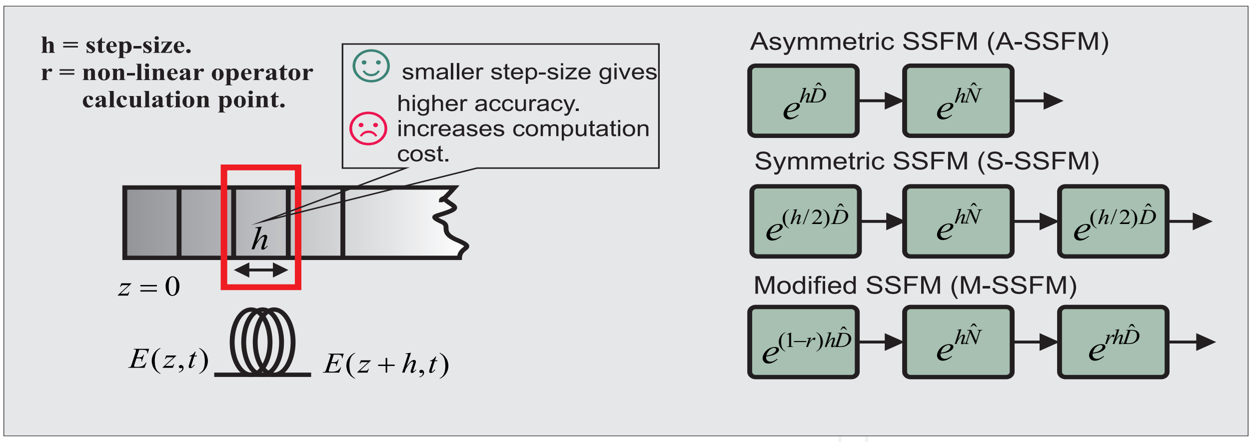


Fig. 4. Comparison of the split-step Fourier methods (SSFM).

(Du et al., 2010). Also that non-linearities behave differently for diverse input parameters of transmission i.e. input power and modulation formats. So we have to modify $Nlpt$ (0≤r≤0.5) along with the optimization of dispersion $D$ and non-linear coefficient $\gamma$, used in the DBP, to get the optimum system performance. It is also well known in the SSFM literature that the linear section $\hat{D}$ of the two subsequent steps can be combined to reduce the number of Fourier transforms. This modified split-step Fourier method (M-SSFM) can mathematically be given as in Eq. 15.

$$E(z+h,t) = exp\Big((1-r)h\hat{D}\Big)exp\big(h\hat{N}\big)exp\Big((r)h\hat{D}\Big) \cdot E\big(z,t\big) \qquad (15)$$

### 3.2.3 Filtered split-step Fourier method (F-SSFM)

In (Du et al., 2010), the concept of filtered DBP (F-DBP) is introduced along with the optimization of non-linear operator calculation point. It is observed that during each DBP step intensity of the out-of-band distortion becomes higher. The distortion is produced by high-frequency intensity fluctuations modulating the outer sub-carriers in the non-linear sections of DBP. This limits the performance of DBP in the form of noise. To overcome this problem a low pass filter (LPF), as shown in Fig.5, is introduced in each DBP step. The digital LPF limits the bandwidth of the compensating waveform so we can optimize the compensation for the low frequency intensity fluctuations without overcompensating for the high-frequency intensity fluctuations. This filtering also reduces the required oversampling factor. The bandwidth of the LPF has to be optimized according to the DBP stages used to compensate fiber transmission impairments i.e bandwidth is very narrow when very few BP steps are used and bandwidth increases accordingly when more DBP stages are used. By using F-SSFM (Du et al., 2010), the results depict that with four backward propagation steps, the Q at the optimal launch power was improved by 2 dB and 1.6 dB for single wavelength CO-OFDM and CO-QPSK systems, respectively, in a 3200 km (40x80km) single-mode fiber link, with no optical dispersion compensation.

### 3.2.4 Logarithmic split-step Fourier method (L-SSFM)

As studies from (Asif et al., 2011) introduces the concept of logarithmic step-size based DBP (L-DBP) using split-step Fourier method. The basic motivation of implementing logarithmic step-size relates to the fact of exponential decay of signal power and thus NL phase shift in the beginning sections of each fiber span as shown in Fig 6. First SSFM methods were based

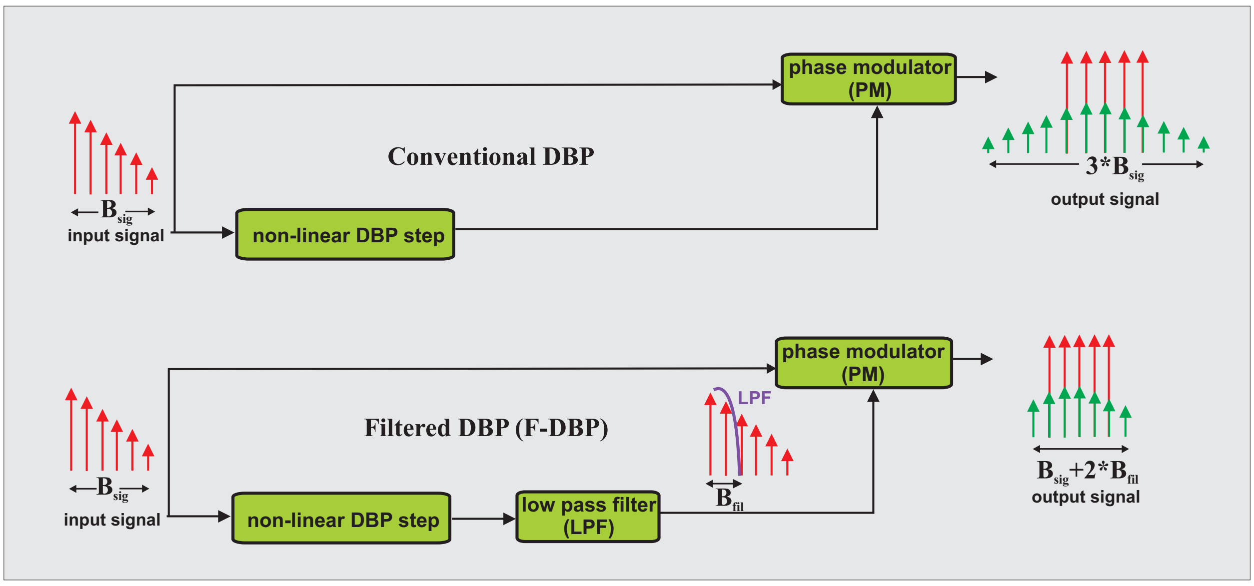


Fig. 5. Block diagram comparing the filtered DBP (F-DBP), conventional DBP schemes and also the bandwidth spectrum ($B$) at different locations of DBP steps (Du et al., 2010).

on the constant step-size methods. Numerical solution of NLSE using SSFM with constant step-size may cause the spurious spectral peaks due to fictitious four wave mixing (FWM). To avoid this numerical artifact and estimating the non-linear phase shift with high accuracy in fewer computations by SSFM, (Bosco et al., 2000; Sinkin et al., 2003) suggest a logarithmic step-size distribution for forward propagation simulations as given in Eq. 16.

$$h_n = -\frac{1}{A\Gamma} ln \left[ \frac{1 - n\sigma}{1 - (n-1)\sigma} \right], \sigma = [1 - exp(-2\Gamma L)] / K \tag{16}$$

Whereas, $L$ is the fiber span length, $\Gamma$ is the loss coefficient and $K$ is the number of steps per fiber span. So logarithmic step-size DBP based on the aforementioned equation is an obvious improvement of DBP. Note that the slope coefficient ($A$) for logarithmic distribution has been chosen as 1 to reduce the relative global error and also for L-DBP 2 minimum iterations are needed to evaluate the logarithmic step-size based DBP stage.

In (Asif et al., 2011), this L-DBP algorithm is evaluated for three different configurations: (a) 20 channel 56Gbit/s (14GBaud) with 25GHz channel spacing; (b) 10 channel 112Gbit/s (28GBaud) with 50GHz channel spacing and (c) 5 channel 224Gbit/s (56GBaud) with 100GHz channel spacing. So that each simulation configuration has the bandwidth occupancy of 500GHz. The DP-QPSK signals are transmitted over 2000km fiber. The algorithm shows efficient compensation of CD and NL especially at higher baud rates i.e. 56GBaud. For this baud rate the calculation steps per fiber span are also reduced from 8 to 4 as compared to the conventional DBP method. The non-linear threshold point (NLT) is improved by 4dB of signal power. One of the main strengths of the this algorithm is that L-DBP eliminates the optimization of DBP parameters, as the same forward propagation parameters can be used in L-DBP and calculation steps per fiber span are reduced up to 50%.

### 3.3 Future step-size distribution concepts

The global accuracy and computational efforts to evaluate the SSFM method mainly depends on the step-size ($h$) selection (Sinkin et al., 2003). In this article several step-size methods are

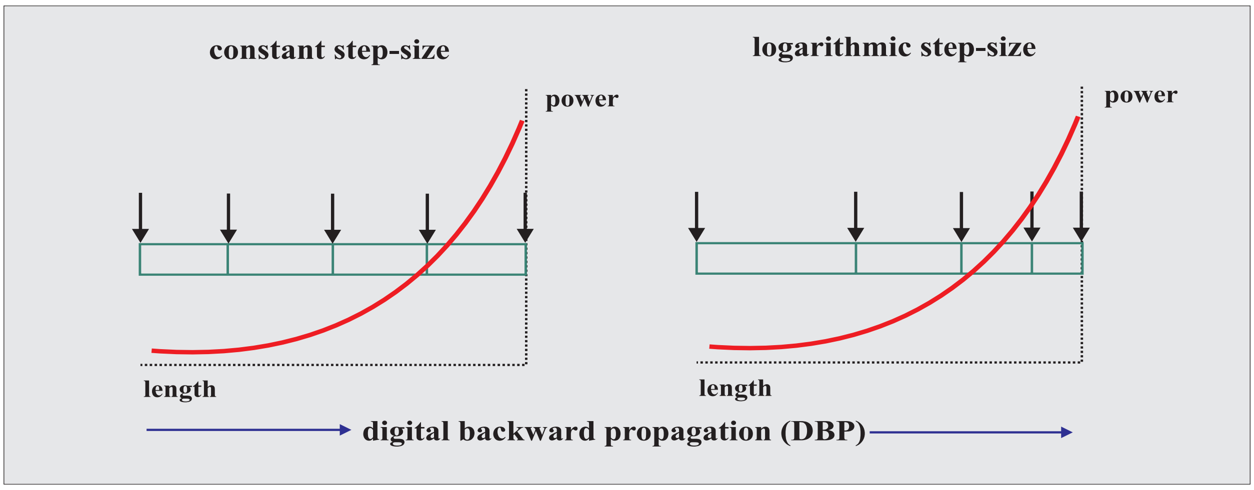


Fig. 6. Comparison of DBP algorithms based on constant step-size method and logarithmic step-size method. The red curves show the power dependence along per-span length.

discussed for forward simulation of optical communication systems. These techniques can be investigated to implement DBP in future. In this section we will discuss the figure of merit for different step-size distribution techniques.

#### 3.3.1 Non-linear phase rotation method

In this method step-size is chosen so that the phase change due to non-linearities $\phi_{NL}$ does not exceed a certain limit (Sinkin et al., 2003). In Eq. 9 the effect of non-linear operator ($\hat{N}$) is to increase the non-linear phase shift $\phi_{NL}$ for a specific step-size ($h$) by an amount as given in Eq. 17.

$$\phi_{NL} = \gamma |E|^2 h \tag{17}$$

An upper-limit for the phase rotation $\phi_{NL}^{max}$ is ensured for this method is the step-size $h$ fulfills Eq. 18.

$$h \leq \frac{\phi_{NL}^{max}}{\gamma |E|^2} \tag{18}$$

This step-size selection method is mainly used for soliton transmission.

#### 3.3.2 Walk-off method

Walk-off method of implementing SSFM is suitable for investigating the WDM (Mateo et al., 2010) transmission systems. In these systems the wavelengths cover a braod spectrum due to which the interplay of chromatic dispersion and intra-channel cross phase modulation (XPM) plays dominant degradation role in system performance. In this method step-size is determined by the largest group velocity difference between channels. The basic intention is to choose the step size to be smaller than a characteristic walk-off length. The walk off length is the length of fiber required for the interacting channels to change their relative alignment by the time duration that characterizes the intensity changes in the optical signals. This length can be determined as: $L_{wo} \approx \triangle t / (D \triangle \lambda)$, where $D$ is chromatic dispersion and $\triangle\lambda$ is the channel spacing between the interacting channels.

In a WDM transmission with large dispersion, pulses in different channels move through each other very rapidly. To resolve the collisions (Sinkin et al., 2003) between pulses in different channels the step-size in the walk-off method is chosen, so that in a single step two pulses in the two edge channels shift with respect to each other by a time that is a specified fraction of the pulse width. Mathematically it is depicted as in Eq. 19.

$$h = \frac{C}{\triangle v_g} \tag{19}$$

Whereas, C is a error bounding constant that can vary from system to system, $\triangle v_g$ is the largest group velocity difference between the channels. In any transmission model $\triangle v_g$=$|D|\Delta\lambda_{i,j}$. Where $\lambda_{i,j}$ is the wavelength difference between channels $i$ and $j$. If the transmission link consists of same kind of fiber, step-size selection due to walk-off method is considered as constant (Sinkin et al., 2003).

### 3.3.3 Local error method

Local error method adaptively adjusts the step-size for required accuracy. In this method step-size is selected by calculating the relative local error $\delta_L$ of non-linear phase shift in each single step (Sinkin et al., 2003), taking into account the error estimation and linear extrapolation. The local error method provides higher accuracy than constant step-size SSFM method, since it is method of third order. On the other hand, the local error method needs additional 50% computational effort (Jaworski, 2008) comparing with the constant step-size SSFM. Simulations are carried out in parallel with coarse step-size ($2h$) and fine ($h$) steps. In each step the relative local error is being calculated: $\delta = \|u_f - u_c\| / \|u_c\|$. Whereas, $u_f$ determines fine solution, $u_c$ is the coarse solution and $\|u\| = \sqrt{|u(t)|^2 dt}$. The step size is chosen by keeping in each single step the relative local error $\delta$ within a specified range $(1/2\delta_G, \delta_G)$, where $\delta_G$ is the global local error. The main advantage of this algorithm is adaptively controlled step size (Jaworski, 2008) .

## 4. Recent developments in DBP

### 4.1 Correlated backward Propagation (CBP)

Recently a promising method to implement DBP is introduced by (Li et al., 2011; Rafique et al., 2011c) which is correlated backward propagation (CBP). The basic theme of implementing this scheme is to take into account the effect of neighbouring symbols in the calculation of non-linear phase shift $\phi_{NL}$ at a certain instant. The physical theory behind CBP is that the SPM imprinted on one symbol is not only related to the power of that symbol but also related to the powers of its neighbouring symbols because of the pulse broadening due to linear distortions. The schematic diagram of the CBP is as given in Fig. 7.

The correlation between neighbouring symbols is taken into account by applying a time-domain filter (Rafique et al., 2011c) corresponding to the weighted sum of neighbouring symbols. Non-linear phase shift on a given symbol by using CBP can be given as in Eq. 20 and 21.

$$E_x^{out} = E_x^{in} \cdot exp\left[-j \cdot \sum_{k=-(N-1)/2}^{+(N-1)/2} c_k \left\{ a\left|E_x^{in}\left(t - k\frac{T_s}{2}\right)\right|^2 + b\left|E_y^{in}\left(t - k\frac{T_s}{2}\right)\right|^2 \right\}\right] \tag{20}$$

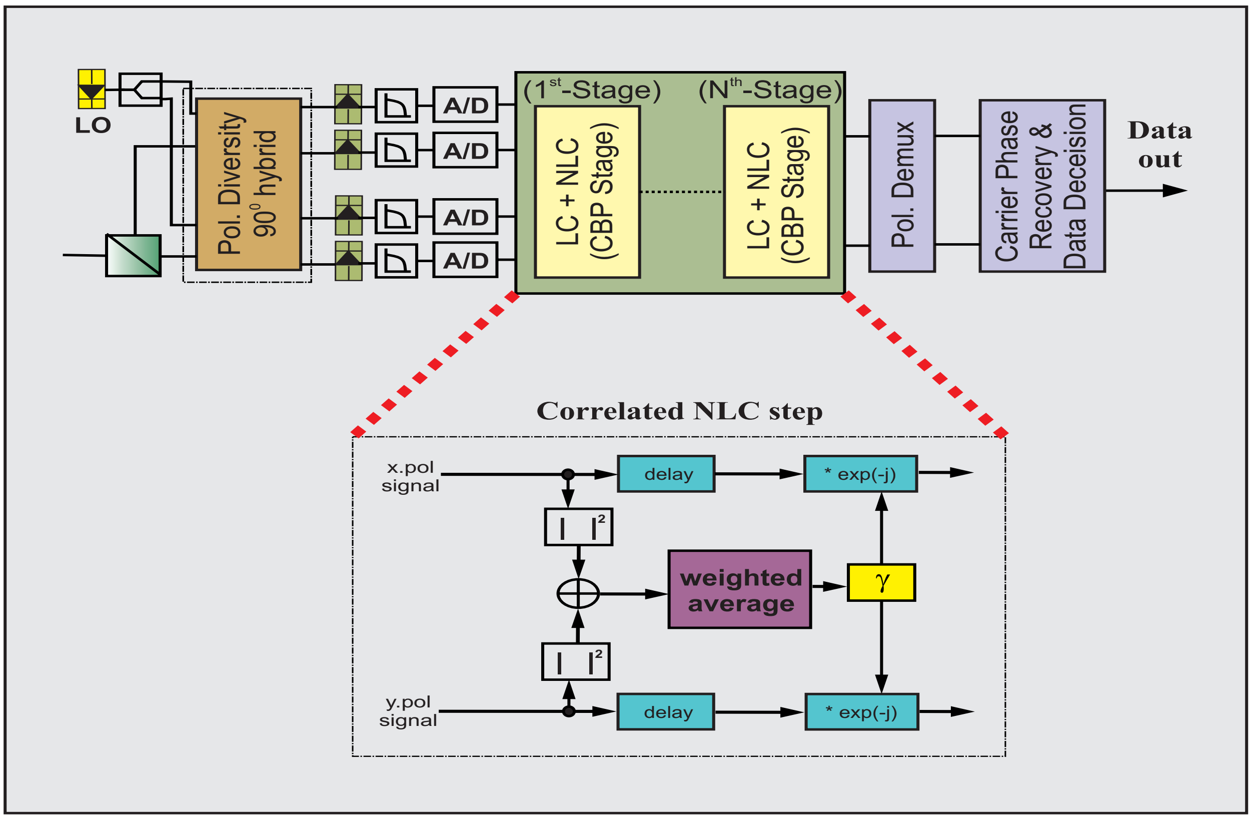


Fig. 7. Block diagram of coherent receiver with correlated backward propagation module (CBP) (Li et al., 2011; Rafique et al., 2011c).

$$E_y^{out} = E_y^{in} \cdot exp\left[-j \cdot \sum_{k=-(N-1)/2}^{+(N-1)/2} c_k \left\{ a \left| E_y^{in}\left(t - k\frac{T_s}{2}\right)\right|^2 + b \left| E_x^{in}\left(t - k\frac{T_s}{2}\right)\right|^2 \right\}\right] \tag{21}$$

Whereas, $E$ is the electric field envelope of the orthogonal polarization states, a and b represent intra-polarization and inter-polarization parameters (Oda et al., 2009), $N$ represents the number of symbols to be considered for a non-linear phase shift, $c_k$ is the weighing vector, $K$ is the delay order, and $T_s$ is the symbol period. In (Li et al., 2011) the investigations depict the results in 100GHz channel spaced DP-QPSK transmission and multi-span DBP shows a reduction of DBP stages upto 75%. While in (Rafique et al., 2011c) the algorithm is investigated for single channel DP-QPSK transmission. In this article upto 80% reduction in required back-propagation stages is shown to perform non-linear compensation in comparison to the standard back-propagation algorithm. By using this method the number of DBP stages are significantly reduced.

### 4.2 Optical backward Propagation (OBP)

The DBP improves the transmission performance significantly by compensating dispersion and non-linearities. However, it requires a considerable amount of computational resources as described in previous sections thus upto now no real time experimental implementations are reported. In (Kumar et al., 2011) an alternative technique for real-time implementation is proposed in optical domain, realized by an effective non-linear coefficient using a pair of highly non-linear fibers (HNLFs). In this method the linear compensation is realized by using

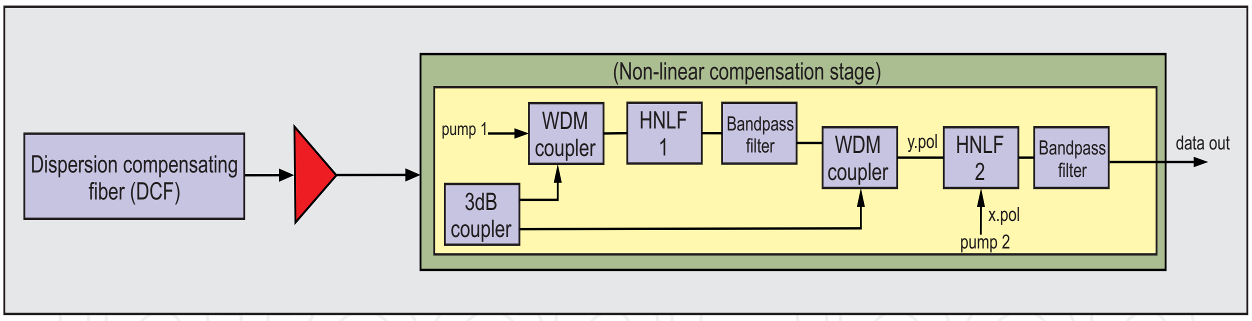


Fig. 8. Block diagram of optical backward propagation module (OBP) (Kumar et al., 2011).

dispersion compensation fibers (DCFs) and non-linear compensation by using HNLFs, as shown in Fig. 8. In this article the technique is evaluated for 32QAM modulation transmission with 25G-symbols/s over 800km fiber. The transmission reach without OBP (but with the DCF) is limited to 240km at the forward error correction limit of 2.1x$10^{-3}$. This is because the multilevel QAM signals are highly sensitive to fiber non-linear effects. The maximum reach can be increased to 640km and 1040km using two-span OBP (multi-span backward propagation) and one-span OBP (per-span backward propagation), respectively.
This technique is still in the early stages of development. As DCF in the OBP module can add additional losses and limit the performance of backward propagation algorithm, as a matter of fact we have to keep launch power to the DCF low so that the non-linear effects in the DCF can be ignored.

## 5. Analysis of step-size selection in 16-QAM transmission

In this section we numerically review the system performances of different step-size selection methods to implement DBP. We apply a logarithmic distribution of step sizes and numerically investigate the influence of varying step size on DBP performance. This algorithm is applied in a single-channel 16-QAM system with bit rate of 112Gbit/s over a 20x80km link of standard single mode fiber without in-line dispersion compensation. The results of calculating the non-linearity at different positions, including symmetric, asymmetric, and the modified (**?**) schemes, are compared. We also demonstrate the performance of using both logarithmic step sizes and constant step sizes, revealing that use of logarithmic step sizes performs better than constant step sizes in case of applying the same number of steps, especially at smaller numbers of steps. Therefore the logarithmic step-size method is still a potential option in terms of improving DBP performance although more calculation efforts are needed compared with the existing multi-span DBP techniques such as (Ip et al., 2010; Li et al., 2011). Similar to the constant step-size method, the logarithmic step-size methods is also applicable to any kind of modulation formats.

### 5.1 DBP algorithms and numerical model

Fig. 9, illustrates the different SSFM algorithms used in this study for a span compensated by 4 DBP-steps. The backward propagation direction is assumed from the left to the right, as the dashed arrows show. For the constant step-size scheme, step size remains the same for all steps, while for the logarithmic step-size scheme, step size increases with decreasing power. The basic principle is well known from the implementation of SSFM to calculate signal propagation in optical fibers, where adaptive step size methods are widely used. As signal

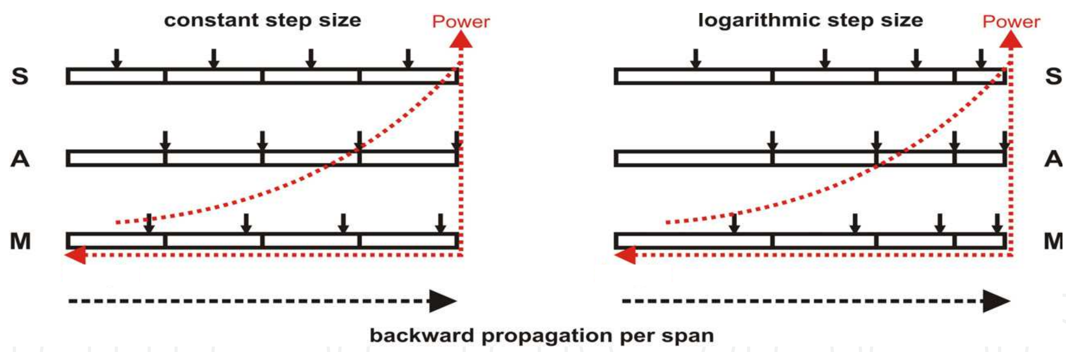


Fig. 9. Schemes of SSFM algorithms for DBP compensation. S: Symmetric-SSFM, A: Asymmetric-SSFM, and M: Modified-SSFM. The red-dotted curves show the power dependence along per-span length..

power exponentially decays along each fiber span, the step size is increased along the fiber. If backward propagation is regarded, the high power regime locates in the end of each span, illustrated in Fig. 1 by the red dotted curves and the step size has to be decreased along each backward propagation span.

Note that the slope coefficient for logarithmic step-size distribution (see section 3.2.4 of this chapter) has been chosen as 1 to reduce the relative global error according to (Jaworski, 2008). The solid arrows in Fig. 9 depict the positions for calculating the non-linear phase. For the symmetric scheme, the non-linearity calculating position (NLCP) is located in the middle of each step. For the asymmetric scheme, NLCP is located at the end of each step. For the modified scheme, NLCP is shifted between the middle and the end of each step and the position is optimized to achieve the best performance (**?**). In all schemes, the non-linear phase was calculated by $\phi_{NL} = \gamma_{DBP} \cdot P \cdot L_{eff}$, where the non-linear coefficient for DBP $\gamma_{DBP}$ was optimized to obtain the best performance. All the algorithms were implemented for DBP compensation to recover the signal distortion in a single-channel 16-QAM transmission system with bit rate of 112Gbps (28Gbaud). In this simulation model, we used an 20x80km single mode fiber (SMF) link without any inline dispersion compensating fiber (DCF). SMF has the propagation parameters: attenuation $\alpha$=0.2dB/km, dispersion coefficient $D$=16ps/nm-km and non-linear coefficient $\alpha$=1.2 km$^{-1}$W$^{-1}$. The EDFA noise figure has been set to 4dB and PMD effect was neglected.

### 5.2 Simulation results

Fig. 10, compares the performance of all SSFM algorithms with varying number of steps per span. In our results, error vector magnitude (EVM) was used for performance evaluation of received 16-QAM signals. Also various launch powers are compared: 3dBm (Fig. 10(a)), 6dBm (Fig. 10(b)) and 9dBm (Fig. 10(c)). For all launch powers the logarithmic distribution of step sizes enables improved DBP compensation performance compared to using constant step sizes. This advantage arises especially at smaller number of steps (less than 8 steps per span). As the number of steps per span increases, reduction of EVM gets saturated and all the algorithms show the same performance. For both logarithmic and constant step sizes, the modified SSFM scheme, which optimizes the NLCP, shows better performance than symmetric SSFM and asymmetric SSFM, where the NLCP is fixed. This coincides with the results which have been presented in **?**. However, the improvement given from asymmetric to modified SSFM is almost negligible when logarithmic step sizes are used, which means the NLCP optimization reveals less importance and it is already sufficient to calculate the non-linearity at the end of each step if logarithmic step sizes are used. On the other hand, at higher launch powers, EVM increases and the saturation of EVM reduction happens toward larger number of steps. Note that with 9dBm launch power, the EVM cannot reach values below 0.15 (BER=$10^{-3}$) even if a large number of steps per span is applied.

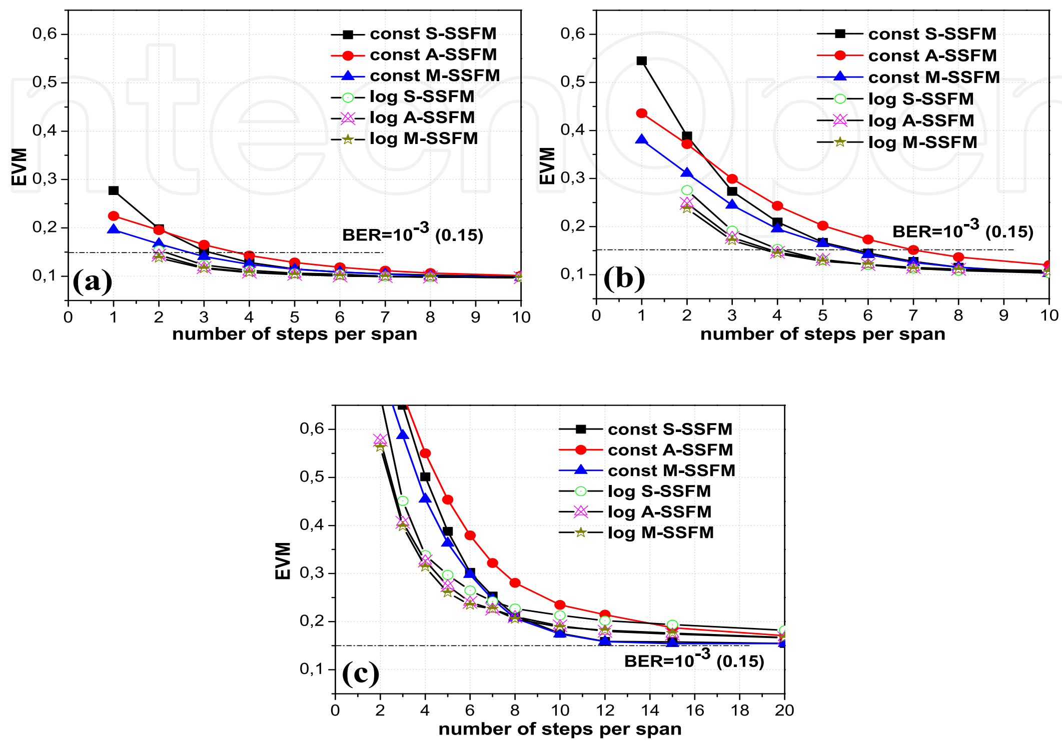


Fig. 10. EVM of all SSFM algorithms with varying number of steps per span for (a) 3dBm, (b) 6dBm and (c) 9dBm.

Fig. 11(a) shows the required number of steps per span to reach BER=$10^{-3}$ at various launch powers for different SSFM algorithms. It is obvious that more steps are required for higher launch powers. Using logarithmic distribution of step sizes requires less steps to reach a certain BER than using uniform distribution of step sizes. At a launch power of 3dBm, the use of logarithmic step sizes reduces 50% in number of steps per span with respect to using the A-SSFM scheme with constant step sizes, and 33% in number of steps per span with respect to using the S-SSFM and M-SSFM schemes with constant step sizes. The advantage can be achieved because the calculated non-linear phase remains constant in every step along the complete. Fig. 11(b) shows an example of logarithmic step-size distribution using 8 steps per span. The non-linear step size determined by effective length of each step, $L_{eff}$, is represented as solid-square symbols and the average power in corresponding steps is represented as circle symbols. Uniformly-distributed non-linear phase for all successive steps can be verified by multiplication of $L_{eff}$ and average power in each step resulting in a constant value. Throughout all simulations the non-linear coefficient for DBP $\gamma_{DBP}$ was optimized to obtain the best performance. Fig. 12 shows constellation diagrams of received 16-QAM signals at 3dBm compensated by DBP with 2 steps per span. The upper diagrams show the results of using constant step sizes with non-optimized $\gamma_{DBP}$ (Fig. 12(a)), and with optimized $\gamma_{DBP}$ (Fig. 12(b)). The lower diagrams show the results of using logarithmic step sizes with non-optimized $\gamma_{DBP}$ (Fig. 12(c)), and with optimized $\gamma_{DBP}$ (Fig. 12(d)). The optimized value is 1.28($km^{-1}W^{-1}$). With optimization of $\gamma_{DBP}$, the constellation diagram can be rotated back completely.

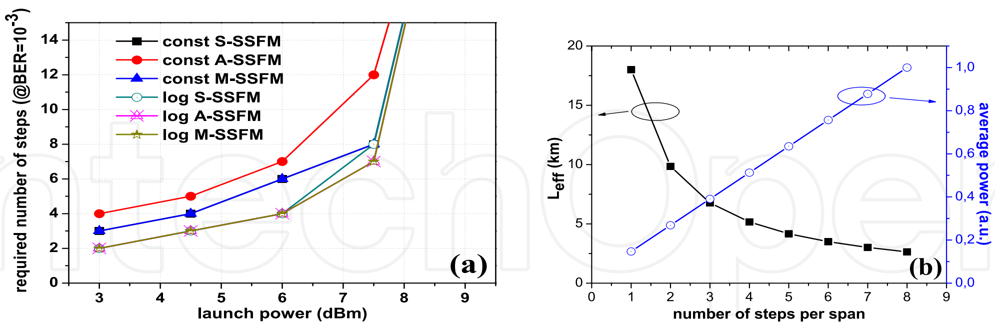


Fig. 11. (a) Required number of steps per span at various launch powers for different SSFM algorithms, and (b) Step-size distribution and average power in each step.

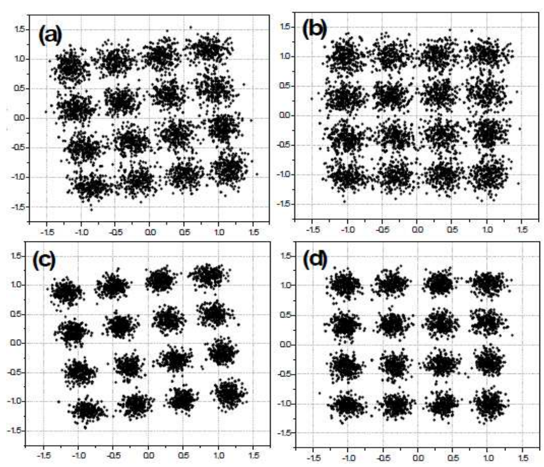


Fig. 12. Constellation diagrams of received 16-QAM signals. (a) constant step size with non-optimized $\gamma_{DBP}$, (b) constant step size with with optimized $\gamma_{DBP}$, (c) logarithmic step sizes with non-optimized $\gamma_{DBP}$ and (d) logarithmic step sizes with optimized $\gamma_{DBP}$.

### 5.3 Conclusion

We studied logarithmic step sizes for DBP implementation and compared the performance with uniform step sizes in a single-channel 16-QAM transmission system over a length of 20x80km at a bit rate of 112Gbit/s. Symmetric, asymmetric and modified SSFM schemes have been applied for both logarithmic and constant step-size methods. Using logarithmic step sizes saves up to 50% in number of steps with respect to using constant step sizes. Besides, by using logarithmic step sizes, the asymmetric scheme already performs nicely and optimizing non-linear calculating position becomes less important in enhancing the DBP performance, which further reduces the computational efforts for DBP algorithms

## 6. Acknowledgement

The authors gratefully acknowledge funding of the Erlangen Graduate School in Advanced Optical Technologies (SAOT) by the German National Science Foundation (DFG) in the framework of the excellence initiative.

## 7. Appendix A

| Method of Implementation | Literature |
|---|---|
| Symmetric split-step Fourier method (S-SSFM) | i) E. Ip et al.: IEEE JLT 2010.<br>ii) C-Y Lin et al.: ECOC 2010.<br>iii) E. Mateo et al.: Opt Express 2010. |
| Asymmetric split-step Fourier method (A-SSFM) | i) E. Ip et al.: IEEE JLT 2008.<br>ii) C-Y Lin et al.: ECOC 2010.<br>iii) D.S Millar et al.: ECOC 2009. |
| Modified split-step Fourier method (M-SSFM) | i) C.Y Lin et al.: ECOC 2010.<br>ii) Du et al.: Opt Express 2010.<br>iii) Asif et al.: Photonics North 2011. |
| Logarithmic split-step Fourier method (L-SSFM) | i) R. Asif et al.: ICTON Conference 2011. |
| Filtered split-step Fourier method (F-SSFM) | i) L. Du et al.: Opt Express 2010. |
| Correlated backward propagation (CBP) | i) L. Li et al.: OFC 2011.<br>ii) Rafique et al.: Opt Express 2011. |

Table 1. Summary of the literature of DBP based on implementation methods.

| Modulation Formats | Literature |
|---|---|
| DPSK, DQPSK and QPSK | i) E. Ip et al.: IEEE JLT 2010.<br>ii) C-Y Lin et al.: ECOC 2010.<br>iii) E. Mateo et al.: App Optics 2009. |
| QAM (4,16,64,256) | i) D. Rafique et al.: Opt Express 2011.<br>ii) S. Makovejs et al.: Opt Express 2010.<br>iii) E. Mateo et al.: Opt Express 2011. |
| POLMUX and WDM (QPSK, QAM) | i) F. Yaman et al.: IEEE J.Phot 2010.<br>ii) E. Mateo et al.: Opt Express 2010.<br>iii) R. Asif et al.: Photonics North 2011. |
| OFDM | i) E. Ip et al.: IEEE JLT 2010.<br>ii) E. Ip et al.: OFC 2011.<br>iii) L. Du et al.: Opt Express 2010. |

Table 2. Summary of the literature of DBP based on modulation formats.

| System Configurations | Literature |
|---|---|
| 10Gbit/s to 40Gbit/s | i) E. Ip et al.: IEEE JLT 2008.<br>ii) C-Y Lin et al.: ECOC 2010.<br>iii) L. Du et al.: Opt Express 2010. |
| $>$ 40Gbit/s till $<$ 100Gbit/s | i) D.S Millar et al.: ECOC 2009.<br>ii) C-Y Lin et al.: ECOC 2010.<br>iii) L. Du et al.: Opt Express 2010. |
| $>$ 100Gbit/s | i) O.S Tanimura et al.: OFC 2009.<br>ii) E. Ip et al.: OFC 2011.<br>iii) E. Mateo et al.: Opt Express 2011.<br>iv) D. Rafique et al.: Opt Express 2011.<br>v) R. Asif et al.: ICTON 2011. |
| WDM (25GHz channel spacing) | i) P. Poggiolini et al.: IEEE PTL 2011.<br>ii) D. Rafique et al.: Opt Express 2011. |
| WDM (50GHz channel spacing) | i) P. Poggiolini et al.: IEEE PTL 2011.<br>ii) R. Asif et al.: ICTON 2011.<br>iii) S. Savory et al.: IEEE PTL 2010. |
| WDM (100GHz channel spacing) | i) P. Poggiolini et al.: IEEE PTL 2011.<br>ii) R. Asif et al.: ICTON 2011.<br>iii) S. Savory et al.: IEEE PTL 2010.<br>iv) E. Mateo et al.: Opt Express 2011. |

Table 3. Summary of the literature of DBP based on system configurations

| Algorithm Complexity | Literature |
|---|---|
| Sub-span step size | i) E. Ip et al.: IEEE/LEOS 2008.<br>ii) G. Li: Adv Opt Photon 2009. |
| Per-span step size | i) E. Ip et al.: IEEE JLT 2008.<br>ii) E. Ip et al.: OFC 2011.<br>iii) S. Savory et al.: IEEE PTL 2010. |
| Multi-span step size | i) L. Li et al.: OFC 2011.<br>ii) D. Rafique et al.: Opt Express 2011.<br>iii) L. Du et .: Opt Express 2011.<br>iv) C-Y Lin et al.: ECOC 2010. |

Table 4. Summary of the literature of DBP based on algorithm complexity

## 8. References


Agrawal, G. (2001). *Fiber-Optic Communication Systems*, John Wiley & Sons Inc, 2nd Edition, New York.

Asif, R., Lin, C.Y., Holtmannspoetter, M. & Schmauss, B. (2010). Optimized digital backward propagation for phase modulated signals in mixed-optical fiber transmission link. *Optics Express*, vol.18, (October 2010) pp.(22796-22807).

Asif, R., Lin, C.Y., Holtmannspoetter, M. & Schmauss, B. (2011). Logarithmic step-size distribution for implementing digital backward propagation in 112Gbit/s DP-QPSK transmission. *12th International Conference on Transparent Optical Networks (ICTON), 2011*, paper Tu.P.6, Stockholm Sweden, June 2011.

Bosco, G., Carena, A., Curri, V., Gaudino, R., Poggiolini, P. & Benedetto S. (2000). Suppression of spurious tones induced by the split-step method in fiber systems simulation. *IEEE Photonics Technology Letters*, vol.12, no.5, (May 2000), pp.(489-491).

Cvecek, K., Sponsel, K., Stephan, C., Onishchukov, G., Ludwig, R., Schubert, C., Schmauss, B., & Leuchs, G. (2008). Phase-preserving amplitude regeneration for a WDM RZ-DPSK signal using a nonlinear amplifying loop mirror. *Optics Express* vol.16, (January 2008), pp.(1923-19289).

Du, L. & Lowery, A. (2010). Improved single channel back-propagation for intra-channel fiber non-linearity compensation in long-haul optical communication systems. *Optics Express*, vol.18, (July 2010), pp.(17075-17088).

Evangelides, S.R., Mollenauer, L., Gordon, J., & Bergamo, N. (1992). Polarization multiplexing with solitons. *IEEE Journal of Lightwave Technology*, vol.10, no.1, (January 1992), pp.(28-35).

Feiste, U., Ludwig, R., Dietrich, E., Diez, S., Ehrke, H.J., Razic, Dz. & Weber, H.G. (1998). 40 Gbit/s transmission over 434 km standard fibre using polarisation independent mid-span spectral inversion. *IET Electronics Letters*, vol.34, no.21, (October 1998), pp.2044-2045.

Fludger, C.R.S., Duthel, T., van den Borne, D., Schulien, C., Schmidt, E., Wuth, T., Geyer, J., De Man, E., Khoe, G.D. & de Waardt, H. (2008). Coherent Equalization and POLMUX-RZ-DQPSK for Robust 100-GE Transmission. *IEEE Journal of Lightwave Technology*, vol.26, no.1, (January 2008) pp.(64-72).

Forghieri, F. (1997). Modeling of wavelength multiplexed lightwave systems. *Optical fiber communication conference (OFC 1997)*, Texas USA, February 1997.

Gavioli, G., Torrengo, E., Bosco, G., Carena, A., Savory, S., Forghieri, F. & Poggiolini, P. (2010). Ultra-narrow-spacing 10-Channel 1.12 Tb/s D-WDM long-haul transmission over uncompensated SMF and NZDSF. *IEEE Photonics Technology Letters*, vol.22, no.19, (October 2010) pp.(1419-1421).

Geyer, J.C., Fludger, C.R.S., Duthel, T., Schulien, C. & Schmauss, B. (2010). Simple automatic non-linear compensation with low complexity for implementation in coherent receivers, *36th European Conference Optical Communication (ECOC), 2010*, paper P3.02, Torino Italy, Sept 2010.

Goldfarb, G. & Li, G. (2007). Chromatic dispersion compensation using digital IIR filtering with coherent detection. *IEEE Photonics Technology Letters*, vol.19, no.13, (JULY 2007), pp.(969-971).

Ip, E. & Kahn, J.M. (2008). Compensation of dispersion and non-linear impairments using digital backpropagation. *IEEE Journal of Lightwave Technology*, vol.26, no.20, (October 2008), pp.(3416-3425).

Ip, E. & Kahn, J.M. (2010). Fiber impairment compensation using coherent detection and digital signal processing. *IEEE Journal of Lightwave Technology*, vol.28, no.4, (February 2010), pp.(502-519).

Iwatsuki, K., Suzuki, K., Nishi, S. & Saruwatari M. (1993). 80 Gb/s optical soliton transmission over 80 km with time/polarization division multiplexing. *IEEE Photonics Technology Letters*, vol.5, no.2, (Febuary 1993) pp. (245-248).

Jansen, S.L., van den Borne, D., Khoe, G., de Waardt, H., Monsalve, C., Splter, S. & Krummrich, P.M. (2005). Reduction of non-linear phase noise by mid-link spectral inversion in a DPSK based transmission system. *Conference on Optical Fiber communication/National Fiber Optic Engineers Conference (OFC/NFOEC) 2005*, paper OThO5, California USA, March 2005.

Jaworski, M. (2008). Step-size distribution strategies in SSFM simulation of DWDM links. *10th International Conference on Transparent Optical Networks (ICTON), 2008*, Athens Greece, June 2008.

Kumar, S. & Yang, D. (2011). Optical backpropagation for fiber-optic communications using highly non-linear fibers. *Optics Letters*, vol.36, (April 2011), pp.(1038-1040).

Li, G. (2009). Recent advances in coherent optical communication. *Advances in Optics and Photonics* vol.1, (February 2009), pp.(279-307).

Li, L., Tao, Z., Dou, L., Yan, W., Oda, S., Tanimura, T., Hoshida, T. & Rasmussen, J. (2011). Implementation efficient non-linear equalizer based on correlated digital back-propagation. *Conference on Optical Fiber communication/National Fiber Optic Engineers Conference (OFC/NFOEC) 2011*, paper OWW3, Los Angeles USA, March 2011.

Li, X., Chen, X., Goldfarb, G., Mateo, E., Kim, I., Yaman, F. & Li, G. (2008) Electronic post-compensation of WDM transmission impairments using coherent detection and digital signal processing. *Optics Express* vol.16, (January 2008), pp.(880-888).

Lin, C.Y., Asif, R., Holtmannspoetter, M. & Schmauss, B. (2010a). Evaluation of nonlinear phase noise in DPSK transmission for different link designs. *Physics Procedia*, vol.5, no.2, (August 2010), pp.(697-701).

Lin, C.Y., Holtmannspoetter, M. , Asif, R. & Schmauss, B. (2010b). Compensation of transmission impairments by digital backward propagation for different link designs, *36th European Conference Optical Communication (ECOC), 2010*, paper P3.16, Torino Italy, Sept 2010.

Marazzi, L., Parolari, P., Martelli, P., Siano, R., Boffi, P., Ferrario, M., Righetti, A., Martinelli, M., Pusino, V., Minzioni, P., Cristiani, I., Degiorgio, V., Langrock, C. & Fejer, M. (2009). Real-time 100-Gb/s polmux RZ-DQPSK transmission over uncompensated 500 km of SSMF by optical phase conjugation. *Conference on Optical Fiber communication/National Fiber Optic Engineers Conference (OFC/NFOEC) 2009*, paper JWA44, California USA, March 2009.

Mateo, E., Yaman, F. & Li, G. (2010). Efficient compensation of inter-channel non-linear effects via digital backward propagation in WDM optical transmission. *Optics Express*, vol.18, (June 2010), pp.(15144-15154).

Mateo, E., Zhou, X. & Li, G. (2011). Improved digital backward propagation for the compensation of inter-channel non-linear effects in polarization-multiplexed WDM systems. *Optics Express*, vol.19, (January 2011), pp.(570-583).

Millar, D.S., Makovejs, S., Behrens, C., Hellerbrand, S., Killey, R., Bayvel, P. & Savory, S.J. (2010). Mitigation of fiber non-linearity using a digital coherent receiver. *IEEE Journal of Selected Topics in Quantum Electronics*, vol.16, no.5, (September 2010) pp.(1217-1226).

Mitra P.P. & Stark J.B. (2001). Non-linear limits to the information capacity of optical fibre communications. *Nature* vol.411 no.6841, (April 2001) pp.(1027-1030).

Mussolin, M., Forzati, M,, Martensson, J., Carena, A. & Bosco, G. (2010). DSP-based compensation of non-linear impairments in 100 Gb/s polmux QPSK. *12th International Conference on Transparent Optical Networks (ICTON), 2010*, paper We.D1.2, Munich Germany, July 2010.

Nelson, L.E. & Kogelnik, H. (2000). Coherent crosstalk impairments in polarization multiplexed transmission due to polarization mode dispersion. *Optics Express*, vol.7, no.10, (November 2000) pp.(350-361).

Nelson, L.E., Nielsen, T. & Kogelnik, H. (2001). Observation of PMD-induced coherent crosstalk in polarization-multiplexed transmission. *IEEE Photonics Technology Letters*, vol.13, no.7, (July 2001), pp.(738-740).

Noe, R., Hinz, S., Sandel, D. & Wust, F. (2001). Crosstalk detection schemes for polarization division multiplexed transmission experiments. *IEEE Journal of Lightwave Technology*, vol.19, no.10, (October 2001), pp.(1469-1475).

Noe, R. (2005). PLL-free synchronous QPSK polarization multiplex/diversity receiver concept with digital I and Q baseband processing. *IEEE Photonics Technology Letters*, vol.17, no.4, (April 2005), pp.(887-889).

Oda, S., Tanimura, T., Hoshida, T., Ohshima, C., Nakashima, H., Zhenning, T. & Rasmussen, J. (2009). 112 Gb/s DP-QPSK transmission using a novel non-linear compensator in digital coherent receiver. *Conference on Optical Fiber communication/National Fiber Optic Engineers Conference (OFC/NFOEC) 2009*, paper OThR6, San-Diego USA, March 2009.

Pardo, O.B., Renaudier, J., Salsi, M., Tran, P., Mardoyan, H., Charlet, G. & Bigo, S. (2011). Linear and nonlinear impairment mitigation for enhanced transmission performance. *Conference on Optical Fiber communication/National Fiber Optic Engineers Conference (OFC/NFOEC) 2011*, paper OMR1, Los Angeles USA, March 2011.

Pare, C., Villeneuve, A., Blanger, P. & Doran, N. (1996). Compensating for dispersion and the nonlinear Kerr effect without phase conjugation. *Optics Letters* vol.21, (September 1996) pp.(459-461).

Poggiolini, P., Bosco, G., Carena, A., Curri, V., Miot, V. & Forghieri, F. (2011). Performance dependence on channel baud-rate of PM-QPSK systems over uncompensated links. *IEEE Photonics Technology Letters*, vol.23, no.1, (January 2011), pp.(15-17).

Rafique, D. & Ellis, A. (2011a). Impact of signal-ASE four-wave mixing on the effectiveness of digital back-propagation in 112 Gb/s PM-QPSK systems. *Optics Express*, vol.19, (February 2011) pp.(3449-3454).

Rafique, D., Zhao, J. & Ellis, A. (2011b). Digital back-propagation for spectrally efficient WDM 112 Gbit/s PM m-ary QAM transmission. *Optics Express*, vol.19, (March 2011), 5219-5224.

Rafique, D., Mussolin, M., Forzati, M., Martensson, J., Chugtai, M. & Ellis, A. (2011c). Compensation of intra-channel nonlinear fibre impairments using simplified digital back-propagation algorithm. *Optics Express*, vol.19, (April 2011), pp.(9453-9460).

Randhawa, R., Sohal, J. & Kaler, R. (2009). Pre-, post and hybrid dispersion mapping techniques for CSRZ optical networks with non-linearities. *Optik - International Journal for Light and Electron Optics*, vol.121, no.14, (August 2010), pp.(1274-1279).

Savory, S., Stewart, A.D., Wood, S., Gavioli, G., Taylor, M.G., Killey, R., & Bayvel, P. (2006). Digital equalisation of 40 Gbit/s per wavelength transmission over 2480 km of standard fibre without optical dispersion compensation. *32nd European Conference Optical Communication (ECOC), 2006*, paper Th2.5.5, Cannes France, September 2006.

Savory, S., Gavioli, G., Killey, R. & Bayvel P. (2007). Electronic compensation of chromatic dispersion using a digital coherent receiver. *Optics Express* vol.15, (March 2007) pp.(2120-2126).

Savory, S., Gavioli, G., Torrengo, E. & Poggiolini, P. (2010). Impact of inter-channel non-linearities on a split-step intra-channel non-linear equalizer, (IEEE Photonics Technology Letters), vol.22, no.10, (May 2010),pp.(673-675).

Sinkin, O.V., Holzlohner, R., Zweck, J. & Menyuk, C.R. (2003). Optimization of the split-step Fourier method in modelling optical-fiber communications systems. *IEEE Journal of Lightwave Technology*, vol.21, no.1, (january 2003), pp. (61-68).

Sponsel, K., Cvecek, K., Stephan, C., Onishchukov, G., Schmauss, B. & Leuchs, G. (2008). Effective negative non-linearity of a non-linear amplifying loop mirror for compensating non-linearity-induced signal distortions. *34th European Conference Optical Communication (ECOC), 2008*, paper Th.1.B5, Brussels Belgium, Sept 2008.

Stephan, C., Sponsel, K., Onishchukov, G., Schmauss, B. & Leuchs G. (2009). Suppression of non-linear phase noise in a DPSK transmission using a non-linear amplifying loop mirror. *Conference on Optical Fiber communication/National Fiber Optic Engineers Conference (OFC/NFOEC) 2009*, paper JthA60, San Diego USA, March 2009.

Taylor, M.G. (2004), Coherent detection method using DSP for demodulation of signal and subsequent equalization of propagation impairments. *IEEE Photonics Technology Letters*, vol.16, no.2, (February 2004), pp. (674676).

Tsang, M., Psaltis, D. & Omenetto, F. (2003). Reverse propagation of femtosecond pulses in optical fibers. *Optics Letters* vol.28, (March 2003), pp.(1873-1875).

Tonello, A., Wabnitz, S. & Boyraz, O. (2006). Duty-ratio control of nonlinear phase noise in dispersion managed WDM transmissions using RZ-DPSK modulation at 10 Gb/s. *IEEE Journal of Lightwave Technology*, vol.24, no.10, (October 2006), pp.(3719-3726).

Winters, J.H. (1990). Equalization in coherent lightwave systems using a fractionally spaced equalizer. *IEEE Journal of Lightwave Technology*, vol.8, no.10, (October 1990), pp.(1487-1491).

Yaman, F. & Li, G. (2009). Non-linear impairment compensation for polarization-division multiplexed WDM transmission using digital backward propagation. *IEEE Photonics Journal*, vol.2, no.5, (August 2009), pp.(144-152).

Yamazaki, E., Sano, A., Kobayashi, T., Yoshida, E. & Miyamoto, Y. (2011). Mitigation of non-linearities in optical transmission systems. *Conference on Optical Fiber communication/National Fiber Optic Engineers Conference (OFC/NFOEC) 2011*, paper OThF1, Los Angeles USA, March 2011.

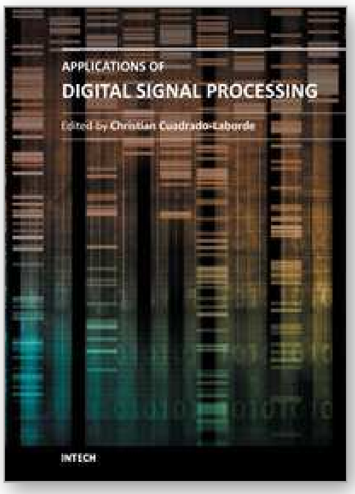


**Applications of Digital Signal Processing**

Edited by Dr. Christian Cuadrado-Laborde

ISBN 978-953-307-406-1
Hard cover, 400 pages
**Publisher** InTech
**Published online** 23, November, 2011
**Published in print edition** November, 2011

In this book the reader will find a collection of chapters authored/co-authored by a large number of experts around the world, covering the broad field of digital signal processing. This book intends to provide highlights of the current research in the digital signal processing area, showing the recent advances in this field. This work is mainly destined to researchers in the digital signal processing and related areas but it is also accessible to anyone with a scientific background desiring to have an up-to-date overview of this domain. Each chapter is self-contained and can be read independently of the others. These nineteenth chapters present methodological advances and recent applications of digital signal processing in various domains as communications, filtering, medicine, astronomy, and image processing.